

Shortest-Path Fractal Dimension for Percolation in Two and Three Dimensions

Zongzheng Zhou¹, Ji Yang¹, Youjin Deng^{1*}, Robert M. Ziff^{2†}

¹*Hefei National Laboratory for Physical Sciences at the Microscale and Department of Modern Physics, University of Science and Technology of China, Hefei, Anhui 230027, PR China and*

²*Michigan Center for Theoretical Physics and Department of Chemical Engineering, University of Michigan, Ann Arbor, Michigan 48109-2136, USA*

(Dated: August 29, 2018)

We carry out a high-precision Monte Carlo study of the shortest-path fractal dimension d_{\min} for percolation in two and three dimensions, using the Leath-Alexandrowicz method which grows a cluster from an active seed site. A variety of quantities are sampled as a function of the chemical distance, including the number of activated sites, a measure of the radius, and the survival probability. By finite-size scaling, we determine $d_{\min} = 1.130\,77(2)$ and $1.375\,6(6)$ in two and three dimensions, respectively. The result in two dimensions rules out the recently conjectured value $d_{\min} = 217/192$ [Phys. Rev. E **81**, 020102(R) (2010)].

PACS numbers: 05.50.+q (lattice theory and statistics), 05.70.Jk (critical point phenomena), 64.60.ah (percolation), 64.60.F- (equilibrium properties near critical points, critical exponents)

I. INTRODUCTION

As a standard model of disordered systems [1, 2], percolation has been intensively studied over the last 50 years and applied to many other fields due to its richness in both mathematics and physics. The nature of the phase transitions in percolation has been well established. In particular, within the two-dimensional (2D) universality class, there are only a few critical exponents left to be expressed exactly, among which is the shortest-path fractal dimension d_{\min} , defined by [2–4]

$$\langle \ell \rangle \sim r^{d_{\min}}, \quad (1)$$

where r is the Euclidean distance between two sites belonging to the same cluster, and ℓ is the shortest path.

The shortest path ℓ between two sites in a cluster is the minimum number of steps on a path of occupied bonds or sites in the cluster, and was first studied independently by several groups in the early 1980s [5–9]. The length ℓ is also called the chemical distance [10]. A related quantity is the spreading dimension d_ℓ [11], which describes the scaling of the mass \mathcal{N} of a critical cluster within a chemical distance ℓ as $\mathcal{N} \sim \ell^{d_\ell}$, and is related to the fractal dimension d_f of the cluster by $d_\ell = d_f/d_{\min}$.

In percolation, the shortest-path naturally occurs during epidemic growth or burning algorithms. Previous measurements of d_{\min} in 2D include $d_{\min} = 1.18(4)$ [6], $1.118(15)$ [7], $1.15(3)$ [10], $1.102(13)$ [12], $1.132(4)$ [13], $1.130(2)$ [14], $1.130\,6(3)$ [15] and $1.1303(8)$ [16]. A summary of the early work is given in Ref. [13].

In 1984, Havlin and Nossal [10] conjectured that $d_{\min} = d_f - 1/\nu = 91/48 - 3/4 = 55/48 = 1.145\,833$, which was soon shown to be too large [13, 14]. In 1987 Larsson [17] speculated that d_{\min} could be $17/16$ or even

1, but these are both excluded. In 1988 Herrmann and Stanley [14] conjectured that $d_{\min} = 2 - d_B + d_{\text{red}}$, where $d_{\text{red}} = 1/\nu = 3/4$ is the “red”-bond dimension and d_B is the backbone dimension. Using Deng, Blöte and Neinhuis’s result $d_B = 1.643\,4(2)$ [18] (see also [19, 20]), we find that this prediction gives $d_{\min} = 2 - 1.643\,4(2) + 0.75 = 1.106\,6(2)$, which is too small. In 1989, Tzschichholz, Bunde and Havlin [21] considered $d_{\min} = 53/48 = 1.104\,166\,6\dots$, which is also below measured values.

In 1998, Porto *et al.* [22] conjectured that d_{\min} is related to a pair-connectivity scaling exponent g_1 by $d_{\min} = g_1 + \beta/\nu$ where $\beta = 5/36$ for 2D. However, g_1 was later shown to have the exact value $g_1 = 25/24$ [15, 23], which implies $d_{\min} = 55/48 = 1.145\,833$, identical to Havlin and Nossal’s earlier conjecture [10].

In 2010, one of us (Y.D.) and coauthors conjectured an exact expression [16] of d_{\min} for the 2D critical and tricritical random-cluster model: $d_{\min} = (g + 2)/(g + 18)/32g$, where g is the Coulomb-gas coupling constant, related to the random cluster fugacity q by $g = (2/\pi) \cos^{-1}(q/2 - 1)$. This conjecture is numerically correct up to the third or fourth decimal place for all values of q studied in Ref. [16]. For the $q \rightarrow 1$ limit—i.e., standard bond percolation—the predicted value $d_{\min} = 217/192 = 1.130\,208$ was consistent with the numerical results in previous works [6, 7, 10, 12–15]. In addition, the conjectured formula exhibits other good properties. It reproduces the exact results for the critical uniform spanning tree ($q \rightarrow 0$) as well as for the tricritical $q \rightarrow 0$ Potts model; at the tricritical $q \rightarrow 0$ point, the derivative with respect to q is also correct.

The main goal of the present work is to carry out a high-precision Monte Carlo test of the conjecture in Ref. [16] in the context of 2D percolation. A numerical estimate of d_{\min} for 3D percolation is also provided. Some preliminary results of this work were reported in a recent paper on biased directed percolation [24].

*Email: yjdeng@ustc.edu.cn

†Email: rziff@umich.edu

II. SIMULATION AND SAMPLED QUANTITIES

We simulate bond percolation on the square and the simple-cubic lattice by the Leath-Alexandrowicz algorithm [6, 25], which grows a percolation cluster starting from a seed site. For each neighboring edge of the seed site an occupied bond is placed with occupation probability p , and the neighboring site is activated and added into the growing cluster. After all the neighboring edges of the seed site have been visited, the growing procedure is continued from the newly added sites. This proceeds until no more new sites can be added into the cluster (the procedure dies out) or the initially set maximum time step ℓ_{\max} is reached.

The above procedure is also called breadth-first growth, and ℓ is equal to the shortest-path length between the seed site and any activated sites at time step ℓ . We set $\ell = 1$ for the beginning of the growth, and measure the number of activated sites $N(\ell)$ as a function of ℓ . In addition, we record the Euclidean distance r_i of each activated site i to the seed site, and define a radius by

$$R(\ell) = \begin{cases} 0 & \text{if } N(\ell) = 0 \\ \sqrt{\sum_{i=1}^N r_i^2} & \text{if } N(\ell) \geq 1 \end{cases} \quad (2)$$

The statistical averages, $\mathcal{N}(\ell) \equiv \langle N(\ell) \rangle$ and $\mathcal{R}(\ell) \equiv \langle R^2(\ell) \rangle^{1/2}$, and the associated error bars are calculated [37]. We also sample the survival probability $\mathcal{P}(\ell)$ that at time step ℓ , the growing procedure still survives.

At criticality, one expects the scaling behavior

$$\mathcal{N}(\ell) \sim \ell^{Y_N}, \quad \mathcal{R}(\ell) \sim \ell^{Y_R}, \quad \mathcal{P}(\ell) \sim \ell^{-Y_P}, \quad (3)$$

where the critical exponents Y_P , Y_N , and Y_R are related to β , ν and d_{\min} by

$$\begin{aligned} Y_N &= \frac{\gamma}{\nu d_{\min}} - 1, & Y_P &= \frac{\beta}{\nu d_{\min}}, \\ 2Y_R &= \frac{\gamma + 2\nu}{\nu d_{\min}} - 1, \end{aligned} \quad (4)$$

with $\gamma = d\nu - 2\beta$ and d equal to the spatial dimensionality. In terms of exponents of epidemic processes [26], these quantities correspond to $\delta = Y_P$, $\eta = Y_N$, and $1/z - \eta/2 = Y_R$.

To eliminate the unknown non-universal constants in front of the scaling behaviors (3), we define the ratio $Q_{\mathcal{O}}(\ell) = \mathcal{O}(2\ell)/\mathcal{O}(\ell)$ for $\mathcal{O} = \mathcal{N}, \mathcal{R}$ and \mathcal{P} . In the $\ell \rightarrow \infty$ limit, one has

$$Y_N = \log_2(Q_{\mathcal{N}}), \quad Y_R = \log_2(Q_{\mathcal{R}}), \quad Y_P = -\log_2(Q_{\mathcal{P}}). \quad (5)$$

In 2D, one has the exactly known exponents $\beta = 5/36$, $\nu = 4/3$, and $\gamma = 43/18$ [1, 27–30]. In 3D, the exact values are unknown, and are numerically found to be $\beta/\nu = 0.4774(1)$ and $\nu = 0.8764(7)$ [31–35].

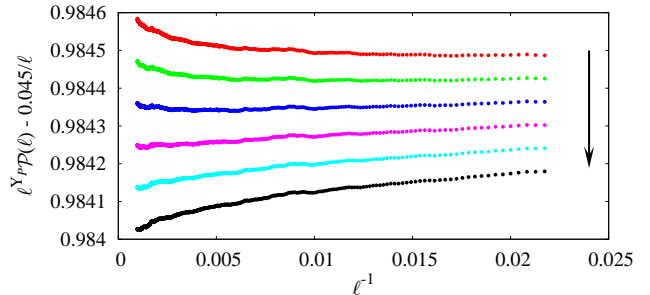


FIG. 1: (Color online) Plot of $\mathcal{P}\ell^{Y_P} - 0.045\ell^{-1}$ versus ℓ^{-1} in 2D. The Y_P value is obtained via Eq. (4) by setting d_{\min} at 1.1302, 1.1304, 1.1306, 1.1308, 1.1310 and 1.1312, following the arrow.

III. INITIAL ESTIMATE OF d_{\min} FOR 2D

We first carried out simulations at the critical point $p = 1/2$ for bond percolation on the square lattice with time step up to $\ell_{\max} = 1024$ and the number of samples about 2×10^9 .

The asymptotic behavior of the observables \mathcal{N} , \mathcal{R} and \mathcal{P} is expected to follow the form

$$\mathcal{O}(\ell) = \ell^Y (a_0 + b_1 \ell^{y_1} + b_2 \ell^{-2}), \quad (6)$$

where higher-order corrections are neglected and the critical exponent Y is given by Eq. (3). The leading finite-size correction exponent is known to be $y_1 = -0.96(6) \approx -1$ [24]. A least-squares criterion was used to fit the data assuming the above form. With y_1 being fixed at -1 , the fit of \mathcal{P} gives $d_{\min} = 1.1308 \pm 0.0002$ and $b_1 = 0.045(5)$, and the fit of \mathcal{N} yields $d_{\min} = 1.1308 \pm 0.0002$.

As an illustration, we plot $\mathcal{P}\ell^{Y_P} - 0.045\ell^{-1}$ in Fig. 1 and $\mathcal{N}\ell^{-Y_N}$ in Fig. 2, both vs. ℓ^{-1} , where the d_{\min} value is set at a series of values in the range [1.1302, 1.1312] in steps of 0.0002, including the above estimate $d_{\min} = 1.1308$. The term $-0.045\ell^{-1}$ is included in Fig. 1 to remove the overall slope seen in the data of \mathcal{P} ; we did not do this to the \mathcal{N} data (Fig. 2), and there the slope is evident. The values of Y_P and Y_N are obtained from Eq. (4), using the exactly known values of β and ν . Because the leading corrections have been subtracted in Fig. 1, it is expected that the curve for the correct d_{\min} value should asymptotically become flat and reach a constant. Figure 1 shows that as ℓ increases, the curve for the conjectured value $217/192 \approx 1.1302$ is bending up while the curve for 1.1312 is bending down. This implies that the correct d_{\min} value should fall somewhere in between. A similar behavior is seen in Fig. 2, where the curve for 1.1308 is approximately straight while those for 1.1302 and 1.1312 are bending down and up, respectively.

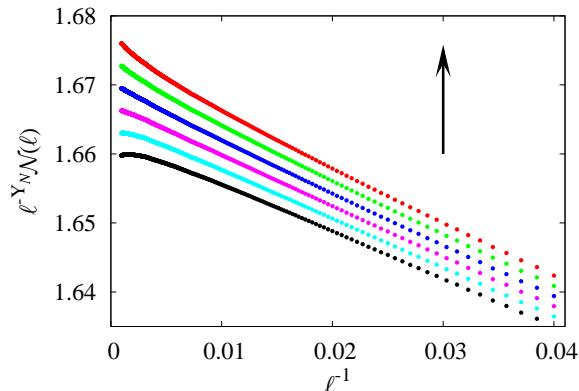


FIG. 2: (Color online) Plot of $\mathcal{N}\ell^{-Y_N}$ versus ℓ^{-1} in 2D. The Y_N value is obtained via Eq. (4) by setting d_{\min} at 1.1302, 1.1304, 1.1306, 1.1308, 1.1310 and 1.1312, following the arrow.

IV. FURTHER SIMULATIONS FOR 2D

Although the conjectured number 217/192 seems to be ruled out by the data shown in Figs. 1 and 2, a more careful analysis is still desirable. The above analysis makes an assumption that the leading correction is governed by ℓ^{-1} , but the physical origin of this term is unclear as the leading irrelevant thermal scaling field has exponent $y_i = -2$. It is conceivable that more slowly convergent corrections exist but are not detected by the simulations up to $\ell_{\max}=1024$. In particular, percolation can be regarded as a special case of biased-directed percolation with the symmetry between spatial and temporal directions restored [24]. In this case, multiplicative and/or additive logarithmic corrections can occur in principle such that the scaling behavior of \mathcal{N} , \mathcal{R} , and \mathcal{P} is modified as

$$\mathcal{O}(\ell) \sim [\log(\ell/\ell_0)]^{y_m} \ell^Y (1 + 1/[\log(\ell/\ell_1)]^{y_c}), \quad (7)$$

where ℓ_0 and ℓ_1 are constants, and y_m and y_c are the associated correction exponents. Corrections of the $\log \log \ell$ form are also possible. We note that due to cancellation between nominator and denominator, the multiplicative logarithmic correction will not explicitly appear in the ratio $Q_{\mathcal{O}}$ ($\mathcal{O} = \mathcal{N}, \mathcal{R}, \mathcal{P}$), for which the scaling behavior is modified as

$$Q_{\mathcal{O}}(\ell) = 2^Y \left(1 + 1/[\log(\ell/\ell_1)]^{y'_c}\right), \quad (8)$$

where y'_c can be equal to y_c or $|y_m|$, depending on the relative amplitudes of the terms associated with them.

To investigate this, we carried out more extensive simulations up to $\ell_{\max} = 16384$. The number of samples was 4.5×10^{10} for $\ell \leq 1024$, 5×10^9 for $1024 < \ell \leq 4096$, 10^9 for $4096 < \ell \leq 8192$, and 3×10^8 for $\ell > 8192$.

From the $Q_{\mathcal{O}}$ data, we calculate the $d_{\min}(\ell)$ value by Eqs. (4) and (5). Table I displays the resulting values of $d_{\min}(\ell)$ from the ratios $Q_{\mathcal{N}}$, $Q_{\mathcal{R}}$ and $Q_{\mathcal{P}}$. It can be

ℓ	$d_{\min}^{(\mathcal{N})}$	$d_{\min}^{(\mathcal{R})}$	$d_{\min}^{(\mathcal{P})}$
12	1.112 909(3)	1.102 251(2)	1.099 42(3)
16	1.117 007(4)	1.109 204(2)	1.106 44(3)
24	1.121 303(4)	1.116 112(2)	1.114 18(3)
32	1.123 540(4)	1.119 588(2)	1.118 10(3)
48	1.125 835(4)	1.123 109(2)	1.122 14(3)
64	1.127 007(4)	1.124 902(2)	1.124 20(3)
96	1.128 215(4)	1.126 743(2)	1.126 32(3)
128	1.128 826(4)	1.127 685(2)	1.127 38(3)
192	1.129 445(4)	1.128 647(2)	1.128 44(3)
256	1.129 755(4)	1.129 140(2)	1.128 99(3)
384	1.130 083(4)	1.129 653(2)	1.129 57(3)
512	1.130 251(4)	1.129 914(2)	1.129 83(3)
768	1.130 42(2)	1.130 180(6)	1.130 15(9)
1024	1.130 49(2)	1.130 317(6)	1.130 36(9)
1536	1.130 58(2)	1.130 455(7)	1.130 33(9)
2048	1.130 63(2)	1.130 532(7)	1.130 27(9)
3072	1.130 70(3)	1.130 61(2)	1.130 5(2)
4096	1.130 68(3)	1.130 62(2)	1.130 6(2)
6144	1.130 72(7)	1.130 65(4)	1.130 9(5)
8192	1.130 80(7)	1.130 72(4)	1.130 8(5)

TABLE I: Results for d_{\min} from $Q_{\mathcal{N}}$, $Q_{\mathcal{R}}$ and $Q_{\mathcal{P}}$ in 2D.

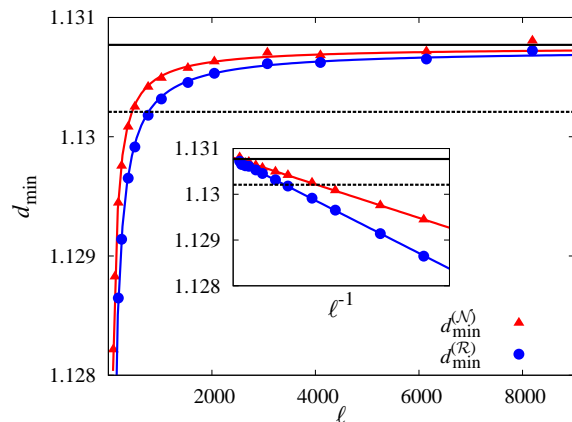


FIG. 3: (Color online) Plot of d_{\min} versus ℓ in 2D, deduced from $Q_{\mathcal{N}}$ and $Q_{\mathcal{R}}$. The inset shows d_{\min} versus ℓ^{-1} . The solid and dashed horizontal lines correspond to $d_{\min} = 1.13077$ and $217/192$, respectively. The red (upper) and blue (lower) curves are obtained from the fits.

clearly seen that for $\ell \leq 3072$, the d_{\min} values that derive from \mathcal{N} and \mathcal{R} increase monotonically as ℓ increases. Further, by looking at the $d_{\min}^{(\mathcal{N})}(L)$ or $d_{\min}^{(\mathcal{R})}(L)$ data for $L = 1024, 2048, 4096L$, one can safely conclude that the asymptotic value d_{\min} is *larger* than 1.1307. For clarity, these data are plotted in Fig. 3. The conjecture $d_{\min} = 217/192$ would mean that the monotonically increasing curves for $d_{\min}^{(\mathcal{N})}$ and $d_{\min}^{(\mathcal{R})}$ must bend downward as ℓ become larger, and thus a very rapid drop would occur near the origin ($1/\ell \rightarrow 0$) in the inset of Fig. 3, which seems very unlikely. The $d_{\min}^{(\mathcal{P})}$ data are less accurate and not shown in Fig. 3.

	ℓ_{\min}	χ^2	d.o.f	d_{\min}	b_1	b_2	y_1
$d_{\min}^{(\mathcal{N})}$	16	13	15	1.130 759(5)	-0.206(2)	0.15(2)	-0.961(3)
	24	12	14	1.130 764(6)	-0.202(4)	0.12(3)	-0.957(5)
	32	12	13	1.130 763(8)	-0.204(6)	0.13(6)	-0.958(7)
	48	11	12	1.130 766(10)	-0.20(1)	0.1(2)	-0.95(1)
	64	7	11	1.130 780(12)	-0.18(2)	0.4(3)	-0.93(2)
$d_{\min}^{(\mathcal{R})}$	24	20	14	1.130 776(4)	-0.265(2)	-0.19(2)	-0.918(2)
	32	13	13	1.130 771(4)	-0.270(3)	-0.14(3)	-0.922(2)
	48	12	12	1.130 768(5)	-0.273(5)	-0.08(7)	-0.925(4)
	64	10	11	1.130 772(7)	-0.266(7)	-0.2(2)	-0.920(5)
$d_{\min}^{(\mathcal{P})}$	16	8	15	1.130 67(4)	-0.39(2)	0.41(9)	-0.99(1)
	24	8	14	1.130 66(5)	-0.40(4)	0.5(3)	-0.99(2)
	32	8	13	1.130 66(6)	-0.41(5)	0.6(5)	-0.99(3)
	48	8	11	1.130 65(7)	-0.4(1)	0.8(11)	-1.00(5)
	64	8	11	1.130 64(8)	-0.4(2)	1(2)	-1.01(8)

TABLE II: Fitting results of d_{\min} in 2D, for various cutoffs ℓ_{\min} . “d.o.f.” stands for “degrees of freedom.”

We fitted the $d_{\min}(\ell)$ data by

$$d_{\min}(\ell) = d_{\min} + b_1 \ell^{y_1} + b_2 \ell^{-2}, \quad (9)$$

using a least-squares criterion. The data for small $\ell < \ell_{\min}$ were gradually excluded to see how the residual χ^2 changes with respect to ℓ_{\min} . Table II lists the fitting results for $d_{\min}^{(\mathcal{N})}$, $d_{\min}^{(\mathcal{R})}$, and $d_{\min}^{(\mathcal{P})}$. From these fits, we obtain $d_{\min}^{(\mathcal{N})} = 1.130 77(3)$, $d_{\min}^{(\mathcal{R})} = 1.130 77(2)$ and $d_{\min}^{(\mathcal{P})} = 1.130 66(15)$. Note that to account for potential systematic errors, the error bars in these final estimates are taken to be significantly larger than those statistical ones in Table II. Considering the stability of the fit results in Table II, we believe that the estimated error margins are reliable. We note that the coefficient b_2 cannot be determined well in the fits for $\ell_{\min} > 32$. Thus, fits with $b_2 = 0$ were also carried out, and the results agree with our above estimates of d_{\min} .

We also simulated critical site percolation on an $L \times L$ triangular lattice with periodic boundary conditions; this system is known to have zero amplitude of the leading irrelevant scaling field with exponent $y_i = -2$. A row of lattice sites was chosen, and all the occupied sites on this row were assumed to belong to the same cluster. The Leath-Alexandrowicz method was then used to grow the cluster. The chemical radius ℓ of the completed cluster was measured. From the scaling $\ell \sim L^{d_{\min}}$, we determine $d_{\min} = 1.130 7(1)$, also ruling out the conjectured value.

V. RESULTS FOR 3D

We simulated bond percolation on the simple-cubic lattice at the central value of the recently estimated critical point $p = 0.248 811 8(1)$ [35], which is slightly below the previous value of $p = 0.248 812 6(5)$ [36]. The simulation was carried up to $\ell_{\max} = 2048$, with the number of sam-

ℓ	$d_{\min}^{(\mathcal{N})}$	$d_{\min}^{(\mathcal{R})}$	$d_{\min}^{(\mathcal{P})}$
12	1.364 7(2)	1.358 44(8)	1.357 6(4)
16	1.365 4(2)	1.363 14(8)	1.359 7(4)
24	1.366 8(2)	1.367 22(8)	1.363 1(4)
32	1.367 9(2)	1.369 01(9)	1.365 6(4)
48	1.369 4(2)	1.370 69(9)	1.368 4(4)
64	1.370 4(2)	1.371 52(9)	1.369 9(4)
96	1.371 6(2)	1.372 42(9)	1.371 8(4)
128	1.372 3(2)	1.372 94(9)	1.372 8(4)
192	1.373 1(2)	1.373 50(9)	1.373 8(4)
256	1.373 5(2)	1.373 78(9)	1.374 4(4)
384	1.374 1(2)	1.374 19(9)	1.375 0(4)
512	1.374 4(2)	1.374 49(9)	1.375 3(4)
768	1.374 6(2)	1.374 7(2)	1.375 4(5)
1024	1.374 6(3)	1.374 7(2)	1.376 0(5)

TABLE III: Results for d_{\min} from $Q_{\mathcal{N}}$, $Q_{\mathcal{R}}$ and $Q_{\mathcal{P}}$ in 3D.

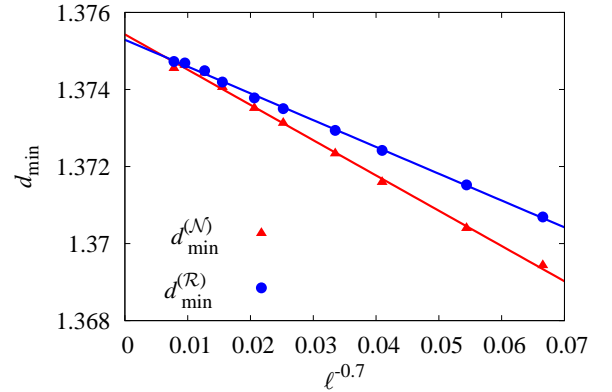


FIG. 4: (Color online) Plot of $d_{\min}^{(\mathcal{N})}$ and $d_{\min}^{(\mathcal{R})}$ versus $\ell^{-0.7}$ in 3D.

	ℓ_{\min}	χ^2	d.o.f	d_{\min}	b_1	b_2	y_1
$d_{\min}^{(\mathcal{N})}$	8	6	11	1.376 1(3)	-0.062(7)	0.50(5)	-0.57(4)
	12	3	10	1.375 7(3)	-0.08(2)	0.7(2)	-0.64(6)
	16	2	9	1.375 6(4)	-0.09(3)	0.9(3)	-0.68(8)
	24	2	8	1.375 4(4)	-0.12(6)	1.4(9)	-0.7(2)
	32	2	7	1.375 3(4)	-0.2(1)	2(2)	-0.8(2)
$d_{\min}^{(\mathcal{R})}$	8	7	11	1.375 4(2)	-0.045(4)	-1.99(3)	-0.60(3)
	12	2	10	1.375 7(3)	-0.035(5)	-1.13(7)	-0.53(5)
	16	2	9	1.375 8(3)	-0.033(6)	-1.2(2)	-0.51(6)
	24	2	8	1.375 7(4)	-0.03(1)	-1.1(3)	-0.52(9)
	32	2	7	1.375 7(4)	-0.04(2)	-0.9(6)	-0.6(2)
$d_{\min}^{(\mathcal{P})}$	8	7	11	1.376 6(4)	-0.19(4)	1.0(2)	-0.80(6)
	12	4	10	1.376 5(5)	-0.23(8)	1.3(5)	-0.8(1)
	16	3	9	1.376 5(5)	-0.2(1)	1.3(9)	-0.8(2)
	24	3	8	1.376 5(7)	-0.2(2)	1(2)	-0.8(3)

TABLE IV: Fitting results of d_{\min} in 3D.

ples 7×10^9 for $\ell \leq 1024$ and 2×10^9 for $\ell > 1024$. Analogous to the procedure on the square lattice, we sampled \mathcal{N} , \mathcal{R} , and \mathcal{P} and studied the ratios $Q_{\mathcal{N}}$, $Q_{\mathcal{R}}$, and $Q_{\mathcal{P}}$. The values of $d_{\min}^{(O)}$ deduced from these ratios with $\beta/\nu = 0.4774(1)$ are listed in Table III. The fitting results are shown in Table IV and yield $d_{\min}^{(\mathcal{N})} = 1.3756(6)$, $d_{\min}^{(\mathcal{R})} = 1.3757(6)$, $d_{\min}^{(\mathcal{P})} = 1.3765(10)$, and $y_1 = -0.7(2)$. The data of $d_{\min}^{(\mathcal{N})}(\ell)$ and $d_{\min}^{(\mathcal{R})}(\ell)$ versus $\ell^{-0.7}$ are further shown in Fig. 4, where the exponent 0.7 reflects the value of y_1 .

VI. CONCLUSION

In conclusion, we determined the shortest-path fractal dimension d_{\min} for percolation in 2D and 3D to be 1.13077(2) and 1.3756(6), respectively. For the 2D value,

we use the result which follows from $\mathcal{R}(\ell)$ and has the smallest error bars. The precision of these numbers is increased compared to the current most accurate values that we are aware of. The conjectured value in 2D, $d_{\min} = 217/192$ [16] is ruled out with a high probability. Grassbergers earlier conjecture $d_{\min} = 26/23$ [3] is also ruled out. The 3D result represents a substantial increase in precision over the previous values of 1.34(1) [14] and 1.374(4) [4].

Y.D. is indebted Alan D. Sokal for valuable discussions. This work was supported in part by NSFC under Grants No. 10975127 and No. 91024026, and the Chinese Academy of Science. R.M.Z. acknowledges support from NSF Grant No. DMS-0553487. The simulations were carried out on the NYU-ITS cluster, which is partly supported by NSF Grant No. PHY-0424082.

-
- [1] D. Stauffer and A. Aharony, *Introduction to Percolation Theory*, 2nd ed. (Taylor and Francis, London, 1994).
- [2] A. Bunde and S. Havlin, in *Fractals and Disordered Systems*, 2nd ed., edited by A. Bunde and S. Havlin (Springer, New York, 1996).
- [3] P. Grassberger, J. Phys. A **25**, 5475 (1992).
- [4] P. Grassberger, J. Phys. A **25**, 5867 (1992).
- [5] P. Grassberger, Math. Biosciences **63**, 157 (1983).
- [6] Z. Alexandrowicz, Phys. Lett. A **80**, 284 (1980).
- [7] R. Pike and H. E. Stanley, J. Phys. A **14**, L169 (1981).
- [8] H. J. Herrmann, D. C. Hong and H. E. Stanley, J. Phys. A **17**, L261 (1984).
- [9] K. M. Middlemiss, S. G. Whittington, and D. S. Gaunt, J. Phys. A **13**, 1835 (1980).
- [10] S. Havlin and R. Nossal, J. Phys. A **17**, L427 (1984).
- [11] J. Vannimenus, J. P. Nadal, and H. Martin, J. Phys. A **17**, L351 (1984).
- [12] R. Rammal, J. C. Angles d'Auriac, and A. Benoit, J. Phys. A **17**, L491 (1984).
- [13] P. Grassberger, J. Phys. A **18**, L215 (1985).
- [14] H. J. Herrmann and H. E. Stanley, J. Phys. A **21**, L829 (1988).
- [15] P. Grassberger, J. Phys. A **32**, 6233 (1999).
- [16] Y. Deng, W. Zhang, T. M. Garoni, A. D. Sokal, and A. Sportiello, Phys. Rev. E **81**, 020102(R) (2010).
- [17] T. A. Larsson, J. Phys. A **20**, L291 (1987).
- [18] Y. Deng, H. W. J. Blöte, B. Nienhuis, Phys. Rev. E **69**, 026114 (2004).
- [19] P. Grassberger, Physica A **262**, 251 (1999).
- [20] J. L. Jacobsen and P. Zinn-Justin, Phys. Rev. E **66**, 055102 (R) (2002).
- [21] F. Tzschichholz, A. Bunde, and S. Havlin, Phys. Rev. A **39**, 5470 (1989).
- [22] M. Porto, S. Havlin, H. E. Roman, and A. Bunde, Phys. Rev. E **58**, 5205(R) (1998).
- [23] R. M. Ziff, J. Phys. A **32**, L457 (1999).
- [24] Z. Zhou, J. Yang, R. M. Ziff and Y. Deng, Phys. Rev. E **86**, 021102 (2012).
- [25] P. L. Leath, Phys. Rev. B **14**, 5046 (1976).
- [26] P. Grassberger and A. de la Torre, Annals Phys. (N.Y.) **122**, 373 (1979).
- [27] J. L. Cardy, Nucl. Phys. B **240**, 514 (1984).
- [28] S. Smirnov, W. Werner, Math. Research Lett. **8**, 729 (2001).
- [29] G. F. Lawler, O. Schramm, W. Werner, Electron. J. Probab. **7**, 2 (2002).
- [30] H. Kesten, Comm. Math. Phys. **109**, 109 (1987).
- [31] Y. Deng and H. W. J. Blöte, Phys. Rev. E **72**, 016126 (2005).
- [32] P. H. L. Martins and J. A. Plascak, Phys. Rev. E **67**, 046119 (2003).
- [33] Y. Tomita and Y. Okabe, J. Phys. Soc. Jpn. **71**, 1570 (2002).
- [34] H. G. Ballesteros, L. A. Fernández, V. Martín-Mayor, A. Muñoz Sudupe, G. Parisi, and J. J. Ruiz-Lorenzo, J. Phys. A **32**, 1 (1999).
- [35] J. Wang, Z. Zhou, and Y. Deng (unpublished).
- [36] C. D. Lorenz and R. M. Ziff, Phys. Rev. E **57**, 230 (1998).
- [37] The definition of \mathcal{R} here is different than that of Ref. [24], where simply the average of R was used. We found that by using the average square radius, a better estimate of d_{\min} was obtained.